Biophysical Chemistry 156 (2011) 153–158

Contents lists available at ScienceDirect

Biophysical Chemistry

journal homepage: http://www.elsevier.com/locate/biophyschem

Energetics of ligand binding to human glutathione transferase A1-1: Tyr-9 associated localisation of the C-terminal helix is ligand-dependent

David Balchin, Heini W. Dirr, Yasien Sayed *

Protein Structure-Function Research Unit, School of Molecular and Cell Biology, University of the Witwatersrand, Johannesburg 2050, South Africa

ARTICLE INFO

Article history:
Received 4 March 2011
Received in revised form 5 April 2011
Accepted 5 April 2011
Available online 12 April 2011

Keywords:
Glutathione transferase
Isothermal titration calorimetry
Heat capacity
Helix 9
Tyrosine 9

ABSTRACT

A C-terminal helix (α9) adjacent to the active site on each subunit is a structural feature unique to the alpha isoform of glutathione transferases which contributes to the catalytic and ligandin functions of the enzyme. The ionisation state of Tyr-9, a residue critical to catalysis, influences α9 dynamics, although the mechanism is poorly understood. In this study, isothermal titration calorimetry was used to probe the binding energetics of G-site (glutathione and glutathione sulfonate) and H-site (ethacrynic acid) ligands to wild-type and a Y9F mutant of human glutathione transferase A1-1. Although previous studies have reported a favourable entropic component to the binding of conjugates occupying both sites, our data reveal that ligand binding is enthalpically driven when either the G- or H-site is occupied independently. Also, heat capacity changes demonstrate that α9 is fully localised by H-site but not G-site occupation. The Tyr-9 hydroxyl group contributes significantly to ligand binding energetics, although the effect differs between the two binding sites. G-site binding is made slightly enthalpically more favourable and entropically less favourable by the Y9F mutation. Binding to the H-site is more dramatically affected, with the K_d for ethacrynic acid increasing 5 fold despite a more favourable ΔS. The heat capacity change is more negative for G-site binding in the absence of the Tyr-9 hydroxyl ($\Delta\Delta C_p = -0.73$ kJ mol^{-1} K^{-1}), but less negative for H-site binding to the Y9F mutant ($\Delta\Delta C_p = 0.63$ kJ mol^{-1} K^{-1}). This suggests that the relationship between Tyr-9 and α9 is not independent of the ligand. Rather, Tyr-9 appears to function in orienting the ligand optimally for α9 closure.

1. Introduction

The cytosolic glutathione transferases (GSTs; EC 2.5.1.18) are important detoxification enzymes in aerobes which catalyse the conjugation of reduced glutathione (GSH) to a range of drugs and toxins [1]. Although diverse in primary sequence, members of the GST superfamily share a common fold and subunit structure characterised by an active site with two distinct binding sites [2–4] (Fig. 1). The G-site is specific for GSH and highly conserved across the GST gene classes, while the H-site can accommodate various hydrophobic, electrophilic substrates. The major catalytic residue in GSTA1-1 is Tyr-9, the hydroxyl group of which functions to activate the GSH thiol for nucleophilic attack on the electrophilic substrate [5]. Previous studies have investigated the binding of a GSH-conjugate (GS-NBD) to Y9F GSTA1-1 using isothermal titration calorimetry [6]. Despite a complete loss of enzyme activity, the conjugate appears to bind more tightly to the mutant enzyme, with the gain in affinity coming at an entropic cost. The structural basis for these thermodynamic effects was suggested by pre-steady state kinetics experiments which show a correlation between the ionisation state of Tyr-9 and α9 localisation that is associated with the binding of GSH-conjugates [7–9]. A C-terminal helix (α9) completing the active site is a structural feature unique to class alpha GSTs (Fig. 1). As shown in Fig. 2, this helix exists in an open conformation in the apo enzyme but becomes localised onto the surface of the protein in crystal structures where the H-site is occupied [10–12]. In the structures shown (Fig. 2), Phe-10 is displaced by Phe-220 when the helix is localised onto the protein surface, and as such is diagnostic of α9 closure. Although not a determinant of protein stability, α9 is critical to both the catalytic and ligandin functions of GSTA1-1 [8,13–15]. The mechanism by which Tyr-9 influences α9 dynamics remains, however, unclear. This study extends our understanding of the role played by the Tyr-9 hydroxyl group in ligand binding to GSTA1-1 and sheds light on the link between Tyr-9 and the closure of α9 over the active site. Isothermal titration calorimetry was used to investigate the energetics of ligand binding to the G-site (glutathione and glutathione sulfonate) and H-site (ethacrynic acid) of both wild-type and Y9F mutant GSTA1-1. By partitioning G- and H-site binding energetics and reporting heat capacity changes for ligand binding, new insight is gained into the structural events accompanying ligand binding in the absence of the Tyr-9 hydroxyl group. Tyr-9-

Abbreviations: α9, C-terminal helix-9 of GSTA1-1; ASA, accessible surface area; $\Delta C_{p,calc}$, the calculated (predicted) change in heat capacity; $\Delta C_{p,obs}$, the observed (experimental) change in heat capacity; EA, ethacrynic acid; G-site, glutathione binding site; GSH, reduced glutathione; GS-NBD, glutathione conjugate with 7-chloro-4-nitrobenzo-2-oxa-1,3-diazole; GSO_3^-, glutathione sulfonate; hGSTA1-1, human class Alpha glutathione transferase with two type one subunits; H-site, hydrophobic electrophilic binding site; ITC, isothermal titration calorimetry.

* Corresponding author. Tel.: +27 11 717 6350; fax: +27 11 717 6351.
E-mail address: Yasien.Sayed@wits.ac.za (Y. Sayed).

0301-4622/$ – see front matter © 2011 Elsevier B.V. All rights reserved.
doi:10.1016/j.bpc.2011.04.005

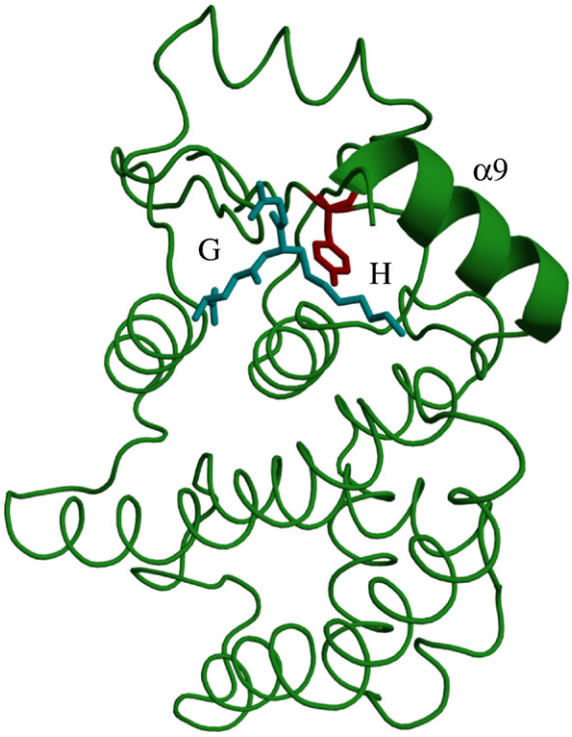

Fig. 1. Subunit structure of GSTA1-1. Tyr-9 and the ligand, *S*-hexylglutathione, are shown as red and cyan sticks respectively. α9 and the G- and H-sites are indicated. (1K3L) [2]. The figure was generated using PyMOL (http://pymol.sourceforge.net/).

induced localisation of α9 was found to be ligand dependent, suggesting that the phenolic hydroxyl group of the active site tyrosine influences α9 dynamics by mediating the orientation of the bound ligand.

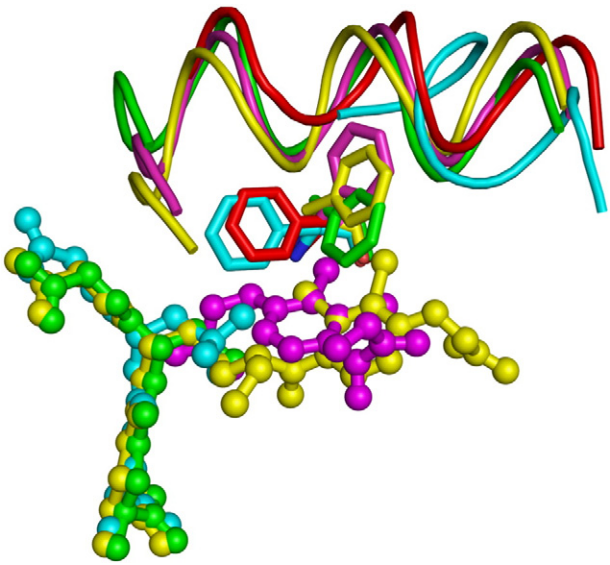

Fig. 2. Active site alignment of GSTA1-1 bound to different ligands. Ligands are depicted in ball-and-stick animation and helix 9 is shown as a ribbon. Red, apo GST (1PKZ) [10]. Green, GST-GSH (1PKW) [10]. Cyan, GST-GSO_3^- (1EV9) [40]. Magenta, GST-EA (1GSF) [11]. Yellow, GST-(EA-GSH conjugate) (1GSE) [11]. Phe-10 is shown in sticks. Note how the position of Phe-10 correlates with the degree of closure of helix-9 over the active site, with the helix more localised (and Phe-10 displaced) in structures where the H-site is occupied.

2. Experimental procedures

2.1. Materials

Reduced glutathione and glutathione sulfonate were from Boehringer-Mannheim (Mannheim, Germany). TCEP (*tris*-(carboxyethyl)-phosphine) and ethacrynic acid were purchased from Sigma-Aldrich (St. Louis, MO, USA). All other reagents were of analytical grade.

2.2. Mutagenesis, protein expression and purification

Wild-type and Y9F human GSTA1-1 proteins were over-expressed using the plasmid pKHA1 [16] in *Escherichia coli* BL21 (DE3) cells containing the pLysS plasmid. The wild-type plasmid was a gift from B. Mannervik (Department of Biochemistry, University of Uppsala, Sweden). The Y9F mutation was incorporated using the QuikChange™ Site-Directed Mutagenesis Kit (Stratagene). The mutant plasmid cDNA was sequenced using an ABI Prism 310 genetic analyser (PE Biosystems) to ensure that no other mutations were present. Wild-type and Y9F mutant proteins were over-expressed and purified using *S*-hexylglutathione affinity chromatography. The bound protein was eluted from the column using 50 mM glycine-NaOH, pH 10 [11]. The purification method described above ensured that the protein was prepared in the absence of ligand (i.e. the apo-form). The proteins were stored in 20 mM sodium phosphate buffer, pH 6.5 containing 0.1 M NaCl, 1 mM EDTA and 0.02% sodium azide. The purity and homogeneity of all protein samples were assessed using SDS-PAGE [17] and SEC-HPLC. Dimeric protein concentrations were determined spectrophotometrically using a molar extinction coefficient of 38 200 M^{-1} cm^{-1} and 35 520 M^{-1} cm^{-1} for the wild-type and mutant, respectively.

2.3. Isothermal titration calorimetry

Calorimetric studies were conducted using a VP-ITC MicroCalorimeter from MicroCal Incorporated. All proteins were prepared in the ligand-free form. The wild-type and Y9F proteins were eluted from the *S*-hexylglutathione affinity column using high pH and subsequently passed through a Sephadex-G25 column. The protein samples were dialysed extensively against 20 mM sodium phosphate buffer, pH 6.5 containing 0.1 M NaCl, 1 mM EDTA, 1 mM TCEP and 0.02% sodium azide. The ligands were prepared in the final dialysate buffer at concentrations of 20 mM, 1.1 mM and 8 mM for GSH, GSO_3^- and ethacrynic acid, respectively. Monomeric protein concentrations of ~0.10 mM wild-type and 0.08 mM Y9F hGSTA1-1 were used for the GSH binding study. The wild-type and Y9F monomeric protein concentration used in the GSO_3^- study ranged between 0.05 mM and 0.06 mM whereas monomeric protein concentrations of ~0.33 mM were used for the ethacrynic acid study. In all the experiments, the ligand (GSH, GSO_3^- or ethacrynic acid) was injected into the ITC sample cell containing protein solution. Computer-controlled injections (3 μl) of ligand into protein solution were carried out until all the binding sites on the protein molecules were saturated. To correct for heats of dilution, control experiments were performed by making identical injections of ligand into the buffer solution. The heat capacity change of the binding reaction was determined from identical experiments performed in the temperature range 5–37 °C. Linked protonation effects were determined by performing identical experiments at 25 °C in a combination of phosphate ($\Delta H_{ion} = 5.12$ kJ mol^{-1}), Pipes (11.45 kJ mol^{-1}), Mes (15.53 kJ mol^{-1}), Mops (21.82 kJ mol^{-1}) and imidazole (36.59 kJ mol^{-1}) buffers [18,19]. Linked protonation effects were calculated using the equation:

$$\Delta H_{obs} = n_H^+ . \Delta H_{ion} + \Delta H_b \quad (1)$$

where ΔH_{obs} is the observed enthalpy of binding, n_H^+ is the number of protons absorbed or released, ΔH_{ion} is the ionisation enthalpy of the buffer and ΔH_b is the net binding enthalpy. No significant changes in

binding affinities in the buffers used above were observed (data not shown).

All raw data from the calorimetric experiments were collected and integrated using the ORIGIN 5 analysis software (MicroCal). For GSH binding, the stoichiometry was fixed to a value of one (N = 1) based on high resolution crystallographic data [10].

2.4. Calculation of ΔC_p values

ASA values were calculated using the NACCESS programme [designed by S.J. Hubbard and J.M. Thornton (1993), Department of Biochemistry and Molecular Biology, University College, London, U.K.] from the structures of GSTA1-1 in complex with GSH (1PKW) [10] and EA (1GSF) [11]. Apo co-ordinates were generated by removing the coordinates for the ligand from the GSH complexed structure in order to avoid errors resulting from using different crystal structures in ASA calculations. Changes in solvent-accessible surface area upon complex formation were estimated as follows:

$$\Delta ASA = ASA_{dimer-ligand} - ASA_{dimer} - ASA_{ligand}. \quad (2)$$

The ΔASA values were converted to expected heat capacity changes by employing the empirical relationship [20–22]:

$$\Delta C_{p,calc} = 2.14 \cdot \Delta ASA_{non-polar} - 0.88 \cdot \Delta ASA_{polar} \quad (3)$$

where the subscripts non-polar and polar represent the change in ASA of non-polar and polar surface area.

3. Results

All thermodynamic parameters for ligand binding are reported in Table 1. The temperature dependence of binding enthalpy for each ligand is illustrated in Fig. 3. ITC thermograms and integrated profiles are shown in the supplementary information accompanying this manuscript for GSH (Fig. S1), GSO_3^- (Fig. S2) and EA (Fig. S3).

3.1. Energetics of ligand binding to wild-type GSTA1-1

Fitting of the integrated ITC profiles indicates that both G-site (GSH, GSO_3^-) and H-site (EA) ligands bind to wild-type hGSTA1-1 with a stoichiometry of one molecule per protein monomer. No evidence of binding cooperativity was observed. The binding of all three ligands is enthalpically driven between 5 and 25 °C. GSH and GSO_3^- binding is entropically favourable below 25 °C and 1.3 °C respectively, whereas no favourable entropic component for EA binding was observed over the temperature range 5–37 °C. Determination of dissociation constants revealed that GSO_3^- binds the G-site about two-orders of magnitude more tightly than GSH and almost 7-fold more tightly than does EA at the H-site. The heat capacity changes are negative and similar for the binding of GSH ($\Delta C_p = -0.44$ kJ mol^{-1} K^{-1}) and GSO_3^- ($\Delta C_p = -0.47$ kJ mol^{-1} K^{-1}), while EA binding results in a more negative ΔC_p (-1.59 kJ mol^{-1} K^{-1}). ITC experiments in four buffers of different ionisation enthalpies revealed that GSH binding is associated with the release of 0.44 protons into the buffer system per protein monomer ($n_H^+ = -0.44$). GSO_3^- binding releases 0.5 protons per monomer into solution ($n_H^+ = -0.50$). EA, in contrast, binds with the concomitant uptake of 2 protons per monomer ($n_H^+ = +2.01$) (Fig. S4).

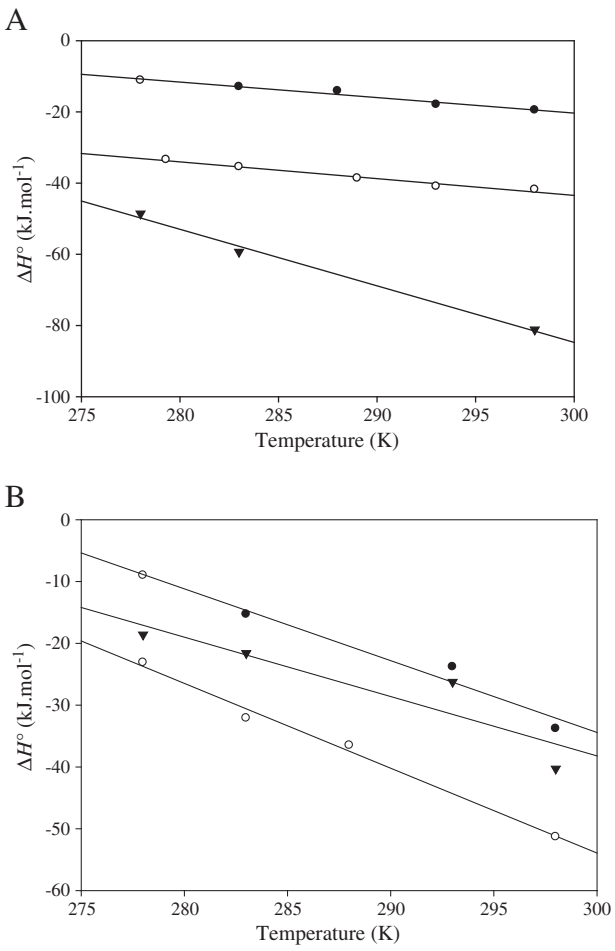

Fig. 3. Temperature dependence of enthalpy of ligand binding to A, wild-type and B, Y9F hGSTA1-1. For the ligands: GSH (●), GSO_3^- (○) and EA (▲).

3.2. GSH binding to Y9F mutant

As with the wild-type protein, GSH binding to the Y9F mutant is enthalpically driven, with entropic contributions favourable below 15.8 °C. At 25 °C, the GSH complex with the mutant is marginally more

Table 1
Thermodynamic parameters for ligand binding to wild-type and Y9F GSTA1-1.

		K_d [a] (μM)	$\Delta G°$ [a]	$\Delta H°$ [a] (kJ mol^{-1})	$T\Delta S°$ [a]	ΔC_p [b] (kJ mol^{-1} K^{-1})	N [d]
Wt	GSH	370 ± 10	−19.6	−19.5 ± 0.3	+0.09	−0.44 ± 0.05	1[c]
	GSO_3^-	4 ± 0.3	−30.8	−41.8 ± 0.6	−10.9	−0.47 ± 0.04	1.0 ± 0.01
	EA	27 ± 2	−26.1	−81.2 ± 0.17	−55.1	−1.59 ± 0.14	1.0 ± 0.003
Y9F	GSH	310 ± 10	−20.1	−33.8 ± 0.6	−13.7	−1.17 ± 0.14	1[c]
	GSO_3^-	11.5 ± 0.7	−28.2	−51.3 ± 1.3	−23.1	−1.38 ± 0.09	1.0 ± 0.02
	EA	150 ± 2.9	−21.8	−40.3 ± 6.7	−18.5	−0.96 ± 0.30	0.7 ± 0.1

[a] Obtained at 25 °C in phosphate buffer.
[b] Obtained between 5 and 25 °C.
[c] Stoichiometry (N) fixed at one molecule of GSH per protein monomer.
[d] Reported errors are from data fitting using the ORIGIN software (MicroCal).

stable than that with the wild-type enzyme, reflected in a lower K_d for the former. Enthalpy is more favourable for GSH binding to the mutant than to wild-type GST ($\Delta\Delta H^\circ = -14.3$ kJ mol^{-1}), although the entropic contribution to binding is less favourable ($T\Delta\Delta S^\circ = -13.79$ kJ mol^{-1}). The Y9F mutation is associated with a more negative ΔC_p for GSH binding than the wild-type.

3.3. GSO_3^- binding to Y9F mutant

Binding of the charged glutathione analogue GSO_3^- to the G-site of the mutant protein is dominated by enthalpically favourable interactions, with entropy contributing favourably only below 9.5 °C. The mutation reduces the affinity of the enzyme for GSO_3^- ($\Delta\Delta G^\circ = 2.6$ kJ mol^{-1}) despite the more favourable ΔH for binding in the absence of the phenolic hydroxyl of Tyr-9. The observed effect on enthalpy is countered by a less favourable entropy change for binding to the mutant. The heat capacity change is more negative than for GSO_3^- binding to the wild-type, with the magnitude of the difference similar to that observed for GSH binding.

3.4. EA binding to Y9F mutant

Although EA binding to the H-site of GSTA1-1 is enthalpically driven for both proteins, the mutation results in a favourable entropic component to binding (below 12 °C) not observed for the wild-type. The mutation also causes a significant destabilisation of the protein complex with EA, manifested in a 5-fold reduction in affinity. The enthalpy of binding is much less favourable for the Y9F mutant at 25 °C when compared to the wild-type enzyme. The entropy change upon binding, however, is markedly more favourable when EA binds to the mutant ($T\Delta\Delta S^\circ = 36.6$ kJ mol^{-1}). Unlike the binding of GSH and GSO_3^-, the interaction of EA with the H-site of the mutant results in a *less* negative ΔC_p than observed for wild-type GSTA1-1.

4. Discussion

Previous studies investigating the energetics of ligand association with class alpha glutathione transferase have focused on the binding of glutathione conjugates and non-substrate ligands to the enzyme [6,23,24]. Here, the thermodynamics of both G-site (glutathione and glutathione sulfonate) and H-site (ethacrynic acid) binding have been characterised comprehensively. In addition, although ligand binding thermodynamics in other GSTs [25–29] have been reported, class alpha is poorly characterised in this respect. Unique to this isoform is a C-terminal helix (α9) which completes the active site and is known to influence the ligandin and catalytic functionality of the enzyme [14]. Insight into the relationship between α9 and ligand binding is therefore an important contribution of this study. Further, the proposed role of Tyr-9 in modulating the dynamics of helix 9 is re-evaluated in light of these new energetics data.

The binding of all three ligands is enthalpically driven. Only GSH binding involves a favourable entropic component and this is minor ($T\Delta S^\circ = +0.09$ kJ mol^{-1}). This stands in contrast to the binding of GSH-conjugates, which is reported to be driven by both enthalpic and entropic effects [30]. This discrepancy suggests that the simultaneous occupation of both the G- and H-sites contributes favourable entropy to binding that is not realised when either the G- or H-site is occupied independently. Considering the large negative entropy change associated with EA binding to the H-site, the source of this favourable entropy is difficult to discern. One possibility is suggested by crystal structures of EA bound at the active site of the protein [11]. These show that EA alone occupies a different conformation at the active site than the EA moiety of EA-GSH conjugates. This conformation (Fig. 4C) might contribute less to active site desolvation than the binding of GSH-complexed EA. The unfavourable entropy change due to ligand and protein ordering (ΔS_{conf}) is therefore overcome by the favourable entropy change that accompanies the liberation of solvent molecules from the active site (ΔS_{solv}).

The determination of linked protonation effects for ligand binding to the wild-type enzyme revealed further disparities between G- and H-site binding. While the binding of G-site ligands results in about 0.5 protons per active site being released into the buffer system, EA binding is accompanied by the uptake of 2 protons per active site. The pK_a values of active site residues are therefore differently affected at each binding site. In the context of this study, it is not possible to unambiguously determine which residues or groups are involved in proton transfer.

The fact that GSH binds much more weakly to the wild-type enzyme than does the other G-site ligand GSO_3^- and the H-site ligand EA, may have physiological relevance. With intracellular concentrations of GSH at approximately 10 mM, GST likely exists in complex with this substrate *in vivo*. A relatively high K_d for GSH would therefore minimise the enthalpic cost associated with product release. The extremely tight binding of the charged glutathione analogue, glutathione sulfonate, is also informative. Although Tyr-9 at the active site of class Alpha GSTs is reported to have an unusually low pK_a [31], our ITC results demonstrate that it is protonated at pH 6.5 since the ionised tyrosinate form would destabilise rather than stabilise the binding of GSO_3^-. Tyr-9, therefore, likely acts as a general acid rather than a general base in catalysis [32]. The tight binding of GSO_3^- relative to GSH is explained by two factors. First, the sulfonate moiety introduces new contacts at the active site, forming two hydrogen bonds with the Tyr-9 hydroxyl and at least one hydrogen bond with the guanidinium group of Arg-15 (Fig. 4A and B). This is reflected in a large negative enthalpic component to binding. Second, unlike that with the physiological substrate GSH, binding energy is not spent activating the thiol group for catalysis.

Substitution of Tyr-9 for a phenylalanine residue does not have a large effect on the overall stability of the enzyme complex with either of the G-site ligands. Differences are, however, observed upon parameterisation of the binding energy. The phenolic hydroxyl of Tyr-9 contributes

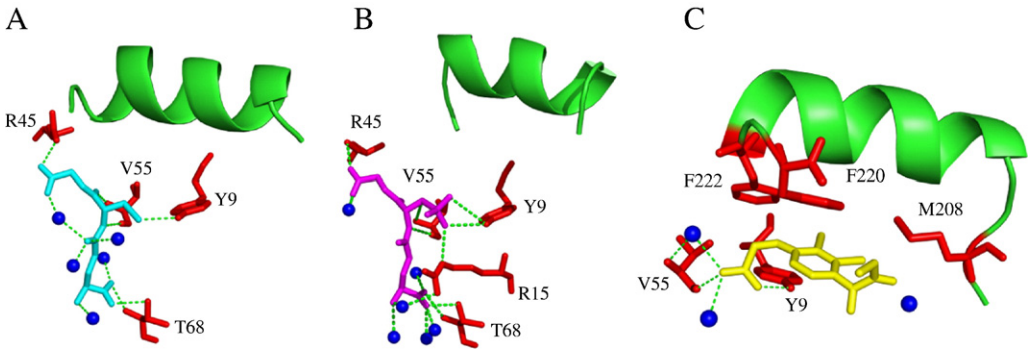

Fig. 4. Protein-ligand interactions at the active site of GST A1-1. *A*, GSH (blue) (1PKW) [10]. *B*, glutathione sulfonate (pink) (1EV9) [40]. *C*, ethacrynic acid (yellow) (1GSF) [11]. Active site residues are shown in red sticks and helix 9 is depicted as a green ribbon. Water molecules are modelled as blue spheres. Potential hydrogen bonds are represented by green dashed lines.

favourably to the entropy of G-site binding but *unfavourably* to binding enthalpy, a surprising result given that the mutation removes a polar group expected to interact with both ligands. This effect may be due to greater solvation of the mutant active site, resulting in favourable contacts being formed between the ligand and water molecules at the expense of solvation entropy.

Changes in heat capacity originate primarily from changes in solvation [20], with the burial of apolar surface reflected by a negative ΔC_p. This observation has been previously applied to the analysis of conformational changes associated with protein–protein [33], protein–DNA [34] and protein–small molecule [35] binding. The heat capacity changes for the binding of a panel of ligands to wild-type hGSTA1-1 have been reported here for the first time, contributing to our understanding of the conformational changes associated with G- and H-site binding. Tertiary interactions are known to lock the amphipathic α9 onto the bulk protein [36,37] (Fig. 4C) and a number of residues in both domains of the protein are within van der Waals distance of the localised helix, including V111, F10, I35, S37, A38, L41, D42, R45 and V55 [38]. α9 localisation is therefore a source of negative heat capacity, and the variation in ΔC_p values for the different ligands likely reflects the varying degrees of α9 closure associated with G- and H-site binding. It is clear from the more negative ΔC_p associated with EA binding, when compared to that for GSH and GSO_3^-, that the C-terminal helix is more localised to the surface of the protein when the H-site is occupied. H-site rather than G-site occupation therefore drives α9 closure. This effect is also apparent in the large, unfavourable ΔS that accompanies EA binding, reflecting the entropic cost associated with α9 localisation (ΔS_{conf}) that is apparently not overcome by desolvation effects. Additional support for this conclusion comes from ΔC_p values predicted from the differences in accessible surface area between the apo and ligand bound forms of the enzyme. The $\Delta C_{p,calc}$ for GSH binding calculated from a crystal structure [10] with α9 removed is -0.41 kJ mol^{-1} K^{-1}, very close to the experimentally determined value. This indicates that α9 is not localised by G-site binding alone. In contrast, the $\Delta C_{p,calc}$ for EA binding (-1.73 kJ mol^{-1} K^{-1}) is comparable to the experimental value in a model where the helix is present. This model is also consistent with structural analyses of ligand binding to the enzyme [10].

Nieslanik and Atkins [6] have demonstrated that the degree of closure of α9 over the active site when a GSH-conjugate binds is coupled to the ionisation state of Tyr-9. However, the mechanism by which Tyr-9 influences the C-terminal helix is unclear, as the phenolic hydroxyl is not within van der Waals distance of any residues in the localised helix [38]. Ibarra et al. [39] have speculated that the Tyr-9 hydroxyl communicates with α9 by modulating an edge-to-face interaction between Tyr-9 and Phe-10. This is proposed to influence the docking of the helix onto the protein via Phe-220 in the helix, which occupies the same space in the ligand-bound enzyme as Phe-10 does in the apo enzyme (Fig. 2). In contrast to previous studies [6,39], we have shown equilibrium energetics data for the binding of ligands which induce α9 localisation to different degrees, giving new insight into the modulation of the helix by Tyr-9. In this regard, the heat capacity changes are most revealing. If Tyr-9, as has been proposed, communicates with α9 via tertiary interactions with other residues in the active site (and not through the ligand), the helix should be less localised in the apo enzyme when these interactions are absent. This interpretation is potentially consistent with our data for the G-site ligands, which show a *more* negative ΔC_p for binding to theY9F mutant than to the wild-type enzyme. In isolation, this could suggest that the mutation causes α9 to assume a conformation that is more open than the open conformation in the apo wild-type. More hydrophobic surface area would therefore be buried upon ligand binding and helix localisation. However, structural (Fig. 2), spectroscopic [40] as well as thermodynamic evidence from this work, indicate that G-site binding does not fully localise α9 to the surface of the protein. Indeed, EA binding, which is known to drive α9 closure, is oppositely affected by the mutation. The *less* negative ΔC_p for H-site binding to the Y9F mutant indicates that the helix fails to localise fully over the active site in the absence of the Tyr-9 hydroxyl. In support of this, the more favourable ΔS and less favourable $\Delta H°$ for EA binding to the mutant are consistent with a more dynamic α9 forming fewer contacts with the protein and bound ligand. The communication between Tyr-9 and α9 is not, therefore, independent of the ligand. Instead, we propose that the Tyr-9 hydroxyl group functions to position the ligand in the correct orientation to drive the closure of α9 over the active site.

Acknowledgements

This work was supported by the University of the Witwatersrand, the South African National Research Foundation Grants 60810, 65510 and 68898, and the South African Research Chairs Initiative of the Department of Science and Technology and National Research Foundation Grant 64788. Any opinion, findings and conclusions or recommendations expressed in this material are those of the authors and therefore the NRF and DST do not accept any liability with regard thereto. YS would like to thank M. Lopez and G. Makhatadze for the use of the ITC machine at Department of Biochemistry and Molecular Biology, Penn State University, College of Medicine, Hershey, Pennsylvania, USA.

Appendix A. Supplementary data

Supplementary data to this article can be found online at doi:10.1016/j.bpc.2011.04.005.

References

[1] R.N. Armstrong, Structure, catalytic mechanism, and evolution of the glutathione transferases, Chem. Res. Toxicol. 10 (1997) 2–18.
[2] I. Le Trong, R.E. Stenkamp, C. Ibarra, W.M. Atkins, E.T. Adman, 1.3-A resolution structure of human glutathione *S*-transferase with *S*-hexyl glutathione bound reveals possible extended ligandin binding site, Proteins 48 (2002) 618–627.
[3] D. Sheehan, G. Meade, V.M. Foley, C.A. Dowd, Structure, function and evolution of glutathione transferases: implications for classification of non-mammalian members of an ancient enzyme superfamily, Biochem. J. 360 (2001) 1–16.
[4] H. Dirr, P. Reinemer, R. Huber, X-ray crystal structures of cytosolic glutathione *S*-transferases. Implications for protein architecture, substrate recognition and catalytic function, EMBO J. 220 (1994) 645–661.
[5] R.W. Wang, D.J. Newton, S.E. Huskey, B.M. McKeever, C.B. Pickett, A.Y. Lu, Site-directed mutagenesis of glutathione *S*-transferase YaYa. Important roles of tyrosine 9 and aspartic acid 101 in catalysis, J. Biol. Chem. 267 (1992) 19866–19871.
[6] B.S. Nieslanik, W.M. Atkins, The catalytic Tyr-9 of glutathione *S*-transferase A1-1 controls the dynamics of the C terminus, J. Biol. Chem. 275 (2000) 17447–17451.
[7] W.M. Atkins, E.C. Dietze, C. Ibarra, Pressure-dependent ionization of Tyr 9 in glutathione *S*-transferase A1-1: contribution of the C-terminal helix to a "soft" active site, Protein Sci. 6 (1997) 873–881.
[8] A. Gustafsson, M. Etahadieh, P. Jemth, B. Mannervik, The C-terminal region of human glutathione transferase A1-1 affects the rate of glutathione binding and the ionisation of the active-site Tyr9, Biochemistry 38 (1999) 16268–16275.
[9] C.A. Ibarra, P. Chowdhury, J.W. Petrich, W.M. Atkins, The anomalous pKa of Tyr-9 in glutathione *S*-transferase A1-1 catalyses product release, J. Biol. Chem. 278 (2003) 19257–19265.
[10] E. Grahn, M. Novotny, E. Jakobsson, A. Gustafsson, L. Grehn, B. Olin, D. Madsen, M. Wahlberg, B. Mannervik, G.J. Kleywegt, New crystal structures of human glutathione transferase A1-1 shed light on glutathione binding and the conformation of the C-terminal helix, Acta Crystallograph. D 62 (2006) 197–207.
[11] A.D. Cameron, I. Sinning, G. L'Hermite, B. Olin, P.G. Board, B. Mannervik, T.A. Jones, Structural analysis of human alpha-class glutathione transferase A1-1 in the apo-form and in complexes with ethacrynic acid and its glutathione conjugate, Structure 3 (1995) 717–727.
[12] Y. Zhan, G.S. Rule, Glutathione induces helical formation in the carboxy terminus of human glutathione transferase A1-1, Biochemistry 43 (2004) 7244–7254.
[13] C.S. Allardyce, P.D. McDonagh, L.-Y. Lian, C.R. Wolf, G.C.K. Roberts, The role of tyrosine-9 and the C-terminal helix in the catalytic mechanism of Alpha-class glutathione *S*-transferase, Biochem. J. 343 (1999) 525–531.
[14] H.W. Dirr, L.A. Wallace, Role of the C-terminal helix 9 in the stability and ligandin function of class alpha glutathione transferase A1-1, Biochemistry 38 (1999) 15631–15640.
[15] L.O. Nilsson, M. Edalat, P.L. Pettersson, B. Mannervik, Aromatic residues in the C-terminal region of glutathione transferase A1-1 influence rate-determining steps in the catalytic mechanism, Biochim. Biophys. Acta 1597 (2002) 157–163.
[16] G. Stenberg, R. Bjornestedt, B. Mannervik, Heterologous expression of recombinant human glutathione transferase A1-1 from a hepatoma cell line, Protein Expr. Purif. 3 (1992) 80–84.
[17] U.K. Laemmli, Cleavage of structural proteins during the assembly of the head of bacteriophage T4, Nature 227 (1970) 680–685.

[18] B.M. Baker, K.P. Murphy, Evaluation of linked protonation effects in protein binding reactions using isothermal titration calorimetry, Biophys. J. 71 (1996) 2049–2055.
[19] H. Fukada, K. Takahashi, Enthalpy and heat capacity changes for the proton dissociation of various buffer components in 0.1 M potassium chloride, Proteins 33 (1998) 159–166.
[20] G.I. Makhatadze, P.L. Privalov, Energetics of protein structure, Advan. Protein Chem. 47 (1995) 307–425.
[21] V.V. Loladze, D.N. Ermolenko, G.I. Makhatadze, Heat capacity changes upon burial of polar and nonpolar groups in proteins, Protein Sci. 10 (2001) 1343–1352.
[22] R.D. Brokx, M.M. Lopez, H.J. Vogel, G.I. Makhatadze, Energetics of target peptide binding by calmodulin reveals different modes of binding, J. Biol. Chem. 276 (2001) 14083–14091.
[23] Y. Sayed, J.A.T. Hornby, M. Lopez, H. Dirr, Thermodynamics of the ligandin function of human class alpha glutathione transferase A1-1: energetics of organic anion ligand binding, Biochem. J. 363 (2002) 341–346.
[24] D. Kolobe, Y. Sayed, H.W. Dirr, Characterisation of bromosulphophthalein binding to human glutathione *S*-transferase A1-1: thermodynamics and inhibition kinetics, Biochem. J. 382 (2004) 1–7.
[25] E. Ortiz-Salmeron, Z. Yassin, M.J. Clemente-Jimenez, F.J. Las Heras-Vazquez, F. Rodriguez-Vico, C. Baron, L. Garcia-Fuentes, A calorimetric study of the binding of S-alkylglutathiones to glutathione *S*-transferase, Biochim. Biophys. Acta 36455 (2001) 1–8.
[26] Z. Yassin, E. Ortiz-Salmeron, M.J. Clemente-Jimenez, C. Baron, L. Garcia-Fuentes, Role of mutation Y6F on the binding properties of Schistosoma japonicum glutathione *S*-transferase, Int. J. Biol. Macromol. 32 (2003) 67–75.
[27] M. Andujar-Sanchez, A.W. Smith, J.M. Clementa-Jimenez, F. Rodriguez-Vico, F.J. Las Heras-Vazquez, V. Jara-Perez, A. Camara-Artigas, Crystallographic and thermodynamic analysis of the binding of *S*-octylglutathione to the Tyr 7 to Phe mutant of glutathione *S*-transferase from Schistosoma japonicum, Biochemistry 44 (2005) 1174–1183.
[28] E. Ortiz-Salmeron, Z. Yassin, M.J. Clemente-Jimenez, F.J. Las Heraz-Vazquez, F. Rodriguez-Vico, C. Baron, L. Garcia-Fuentes, Thermodynamic analysis of the binding of glutathione to glutathione *S*-transferase over a range of temperatures, Eur. J. Biochem. 268 (2001) 4307–4314.
[29] E. Ortiz-Salmeron, M. Nuccetelli, A.J. Oakley, M.W. Parker, M. Lo Bello, L. Garcia-Fuentes, Thermodynamic description of the effect of the mutation Y49F on human glutathione transferase P1-1 in binding with glutathione and the inhibitor S-hexylglutathione, J. Biol. Chem. 47 (2003) 46938–46948.
[30] B.S. Nieslanik, C. Ibarra, W.M. Atkins, The C-terminus of glutathione *S*-transferase A1-1 is required for entropically-driven ligand binding, Biochemistry 40 (2001) 3536–3543.
[31] W.M. Atkins, R.W. Wang, A.W. Bird, D.J. Newton, A.Y.H. Lu, The catalytic mechanism of glutathione *S*-transferase (GST). Spectroscopic determination of the pK_a of Tyr-9 in rat GSTA1-1, J. Biol. Chem. 268 (1993) 19188–19191.
[32] S.W. Huskey, W.P. Huskey, A.Y.H. Lu, Contributions of thiolate "desolvation" to catalysis by glutathione *S*-transferase isozymes 1–1 and 2–2: evidence from kinetic solvent isotope effects, J. Am. Chem. Soc. 113 (1991) 2283–2290.
[33] D.G. Myszka, R.W. Sweet, P. Hensley, M. Brigham-Burke, P.D. Kwong, W.A. Hendrickson, R. Wyatt, J. Sodroski, M.L. Doyle, Energetics of the HIV gp120-CD4 binding reaction, Proc. Natl. Acad. Sci. USA 97 (2000) 9026–9031.
[34] R.S. Spolar, M.T. Record Jr., Coupling of local folding to site-specific binding of proteins to DNA, Science 263 (1994) 777–784.
[35] C.A. McElroy, A. Manfredo, P. Gollnick, M.P. Foster, Thermodynamics of tryptophan-mediated activation of the trp RNA-binding attenuation protein, Biochemistry 45 (2006) 7844–7853.
[36] D.C. Kuhnert, Y. Sayed, S. Mosebi, M. Sayed, T. Sewell, H.W. Dirr, Tertiary interactions stabilise the C-terminal region of human glutathione transferase A1-1: a crystallographic and calorimetric study, J. Mol. Biol. 349 (2005) 825–838.
[37] S. Mosebi, Y. Sayed, J. Burke, H.W. Dirr, Residue 219 impacts on the dynamics of the C-terminal region in glutathione transferase A1-1: implications for stability and catalytic and ligandin functions, Biochemistry 42 (2003) 15326–15332.
[38] C. Ibarra, B.S. Nieslanik, W.M. Atkins, Contribution of aromatic-aromatic interactions to the anomalous pKa of Tyrosine-9 and the C-terminal dynamics of glutathione *S*-transferase A1-1, Biochemistry 40 (2001) 10614–10624.
[39] I. Sinning, G.J. Kleywegt, S.W. Cowan, P. Reinemer, H.W. Dirr, R. Huber, G.L. Gilliland, R.N. Armstrong, X. Ji, P.G. Board, B. Olin, B. Mannervik, T.A. Jones, Structure determination and refinement of human class alpha glutathione transferase A1-1, and a comparison with the mu and pi class enzymes, J. Mol. Biol. 232 (1993) 192–212.
[40] E.T. Adman, I. Le Trong, R.E. Stenkamp, B.S. Nieslanik, E.C. Dietze, G. Tai, C. Ibarra, W.M. Atkins, Localization of the C-terminus of rat glutathione transferase A1-1: crystal structure of mutants W21F and W21F/F220Y, Proteins 42 (2001) 192–200.